

## PIEZOELECTRIC BASED BROADBAND NONLINEAR VIBRATION ENERGY HARVESTER USING MULTIPLE MAGNETS

<sup>1</sup>AG M. ASMUSLIZAN ASNEH, <sup>2</sup>ASAN G.A. MUTHALIF, <sup>3</sup>AZNI N. WAHID, <sup>4</sup>AHMAD JAZLAN,  
<sup>5</sup>NOOR H.H.M HANIF

Smart Structure, Systems and Control Research Laboratory (S<sup>3</sup>CRL)  
Department of Mechatronics Engineering, International Islamic University Malaysia, Jalan Gombak, 53100, Kuala Lumpur,  
Malaysia  
E-mail: <sup>1</sup>mechejan@gmail.com, <sup>2</sup>asan@iium.edu.my

**Abstract** - The advancement of technology has made low-powered devices such as wireless sensor network powered using small battery become possible. However, this type of battery has limited lifespan and needed to be changed frequently which is not convenient when placed in remote area or harsh environment. Therefore, devices that can harvest energy from their surrounding are preferred. One of the famous method is by using piezoelectric transducer to scavenge ambient vibration energy. However, the piezoelectric harvester (PEH) usually has small bandwidth that it can operate. This paper proposed a PEH in the form of cantilever beam with a tip mass along with multiple fixed magnets in certain configuration. The proposed design uses external force by magnet to alter its stiffness and then due the nonlinearity effect introduced by magnets, the operating bandwidth of the PEH is increased. With proper configuration, the proposed design has improved bandwidth compared to PEH without any magnet. It is also found that power output of proposed PEH is relatively higher than conventional PEH which is about 1314  $\mu\text{W}$  where this value is enough to power up low-powered device. In addition, the power per frequency of proposed PEH is 81.59  $\mu\text{W}/\text{Hz}$ , which is about 64 percent higher than the PEH without any magnets.

**Index Terms** - Broadband, Multiple Magnets, Nonlinear, Piezoelectric, Vibration Energy Harvesting

### I. INTRODUCTION

Over the past few decades, energy harvesting technology has become an interesting topic among the researchers especially when it comes to harvesting energy from the environment. Almost everything that we used often required battery to operate[1] thus, battery that has higher life-span is preferable. A self-powered device that can harvest energy from its surrounding is therefore favored by everyone. Energy from the environment can come in the form of thermal energy, radio frequency, magnetic field energy or mechanical vibration energy[2]-[5]. To harvest these kind of energies, transducers are needed and they can be capacitive, electromagnetic or piezoelectric transducers [4]. For this research, piezoelectric transducers are chosen due to their ease-of-use and considered as the best materials to be used in harvesting mechanical vibration energy from environment. Challenges that came when using piezoelectric transducers to harvest vibration energy include increasing the magnitude of power harvested and to broaden its operating frequency. To overcome these limitations, several methods are introduced over the past years; 1) by resonance frequency tuning method, 2) by targeting multimodal energy harvesting method and 3) by nonlinear energy harvesting method.

The first technique which is resonance frequency tuning method tunes the resonance frequency of the system either by using manual or self-tuning approach. One example of the resonance frequency tuning method which is done manually is a design that proposed by [5]. Reference [5] proposed a design where the piezoelectric energy harvester (PEH) is a

cantilever beam-type harvester and coupled with a magnet that fixed on a slider. By adjusting the magnet position, this will affect the stiffness of the whole system since the changes in magnet position will alter the magnetic force experienced by the harvester. For the self-tuning approach, work by [6] proposed a harvester with a magnet where the magnet position can be changed autonomously. The magnet is fixed on a threaded rod and the magnet position is altered by using dc motor. Moreover, the harvester requires 3.2 J to 3.9 J of energy to tune itself. Multimodal energy harvesting method is where it modifies the geometrical design of harvester. The harvester may have multiple cantilever beams. This design can be seen in one of the harvester that proposed by[7]. The harvester is comb-shaped where it consists several cantilever beams with different length. The shape of each beam is also manipulated to improve the performance of the harvester. This method of multimodal energy harvesting also can be seen in harvester designed by [8] and [9]. Another method to improve the performance of harvester when harvesting energy from surrounding using piezoelectric transducer is by using nonlinear energy harvesting approach. Nonlinearities can be brought into the system by using magnet, or by introducing bi-stable conditions to the system or by using mechanical stopper [10]. Some example of using this method to enhance the performance of the harvester is introduced by [11] which not only use magnet but also use a trapezoidal cantilever beam. Work by[12] reported that using external magnet yields 30.8 percent and 60.6 percent increase in open circuit voltage and optimal load power respectively. Another design that utilizes this nonlinear method is PEH

designed by[13]where the harvester is capable of scavenging vibration from three direction.Overall, the resonance frequency tuning method need manual adjustment. Even if it is self-tuned, it still required additional energy to operate. Meanwhile, for multimodal energy harvesting method, it tends to be bulky which is unsuitable for micro-scale devices. On the other hand, by using nonlinear energy harvesting method, the bandwidth of the harvester can be increased easily. With proper configuration, this method can also improve the maximum power output of the harvester.

The focus of this paper is to develop mathematical model representing the PEH and to find the best configuration which can improve the bandwidth of the harvester, lower the resonance frequency so that it will be suitable to be used for small devices, and to enhance the power output of the harvester.The PEH proposed is a cantilever beam type with a tip mass or proof mass.Several fixed magnets are placed at multiple position around the tip mass to influence the stiffness of the harvester. These magnet forces can be in attractive mode or repulsive mode or the combination of two. The simulation study is carried out using MATLAB software.

## II. MATHEMATICAL MODELLING

The fig. 1 shows our model where the piezoelectric patch is attached on aluminum cantilever beam.Three magnets are attached at tip mass so that the harvester stiffness can be altered using magnet from three direction namely top, bottom, and front. The equivalent mechanical model is shown in fig. 2 where the whole system is subjected to base excitation $x_0(t)$ . The system is single-degree of freedom system where its mathematical model can be developed based on mathematical model in[12]. The equation of motion can be given as

$$M_{eq}\ddot{x}(t) + C_{eq}\dot{x}(t) + K_{eq}x(t) + \Theta_b V(t) = -\mu M_{eq}\ddot{x}_0(t) \quad (1)$$

$$I(t) + C^s \dot{V}(t) - \Theta_f \dot{x}(t) = 0. \quad (2)$$

where  $x(t)$ is the relative displacement of proof mass of a cantilever PEH, $M_{eq}$ ,  $C_{eq}$ , and  $K_{eq}$  are equivalent mass, damping and stiffness of the PEH respectively,  $\Theta_f$  and  $\Theta_b$  are forward and backward electromechanical effects respectively while  $\mu$  is amplitude correction factor for improving the model.  $C^s$  is the clamp capacitance of the piezoelectric transducer, and  $V(t)$  is the voltage produce across the piezoelectric element where  $R$  is the load resistance. By observing the equivalent model in fig. 2, due to extra force introduced by magnets, the equation of motion (1) and (2) became

$$M_{eq}\ddot{x}(t) + C_{eq}\dot{x}(t) + K_{eq}x(t) + \Theta_b V(t) + F_m = -\mu M_{eq}\ddot{x}_0(t) \quad (3)$$

$$\frac{V(t)}{R} + C^s \dot{V}(t) - \Theta_f \dot{x}(t) = 0, \quad (4)$$

While  $F_m$  is a force exerted by magnet and it is described as

$$F_m = F_{m1} + F_{m2} + F_{m3} \quad (5)$$

Where  $F_{m1}$ ,  $F_{m2}$ , and  $F_{m3}$  are force due to top, front, and bottom magnet respectively.Force by magnet when it is assumed attractive according to [15] can be written as

$$F_m = -\frac{3\tau_0 m_1 m_2}{2\pi[D_m]^4} \quad (6)$$

Where  $\tau_0$  is permeability of medium,  $m_1$ and  $m_2$  are moment of magnetic dipoles where it can be calculated using (19), and  $D_m$  is distance between the magnets.Then, force due to top magnet can be written as

$$F_{m1} = -\frac{3\tau_0 m_1 m_2}{2\pi[-x(t) + D_t]^4} \quad (7)$$

While force due to bottom magnet can be written as

$$F_{m3} = -\frac{3\tau_0 m_1 m_2}{2\pi[x(t)-D_b]^4}. \quad (8)$$

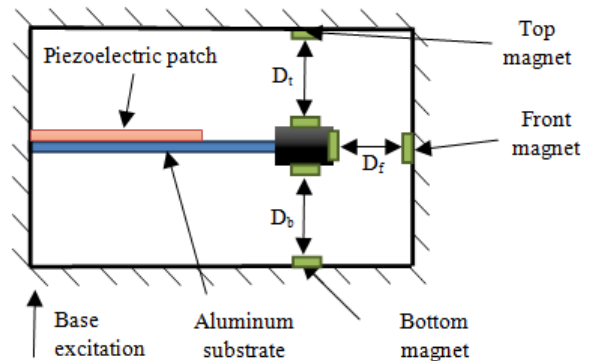


Fig. 1 Proposed design of PEH. There are three fixed magnets, top, bottom, and front magnet.

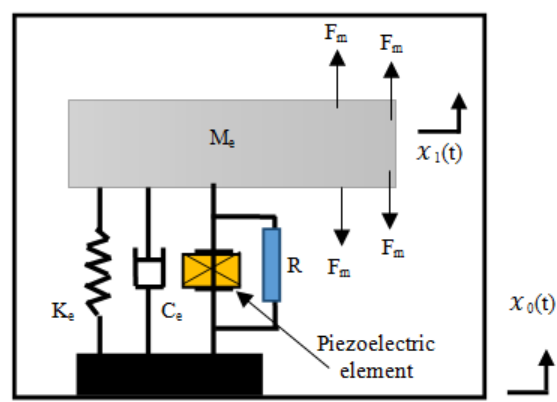
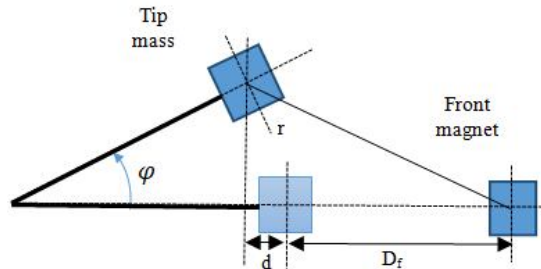


Fig. 2 Equivalent mechanical model of the proposed PEH



**Fig. 3 Geometric diagram of position of front magnet and end most of the cantilever beam**

For force from front magnet, the distance  $d$  need to be calculated first and it can be obtained using

$$d = L_b - L_b \cos \varphi. \quad (9)$$

Then, the distance between front magnet and magnet at tip mass can be calculated using

$$r = \sqrt{(x(t))^2 + (d + D_f)^2}. \quad (10)$$

Therefore, the force due to front magnet is

$$F_{front} = -\frac{3\tau_0 m_1 m_2}{2\pi[r]^4} \quad (11)$$

but this force is a force vector. Therefore, it need to be changed first so the force due to front magnet is along x-direction. The force due to front magnet became

$$F_{m2} = \frac{F_{front} L_b \sin \varphi}{r}. \quad (12)$$

To do the simulation study, the equation of motion that developed is converted into state space representation. The state space representation later solved using ode solver in MATLAB software. The state space representation is

$$\dot{Z}_1(t) = Z_2(t), \quad (13)$$

$$\begin{aligned} \dot{Z}_2(t) &= -\frac{c_{eq}}{M_{eq}} Z_2(t) - \frac{k_{eq}}{M_{eq}} Z(t) - \\ &\quad \frac{\Theta_b}{M_{eq}} V(t) - \mu \ddot{x}_0(t) - F_m, \end{aligned} \quad (14)$$

$$\dot{Z}_3(t) = -\frac{Z_3(t)}{C^s R} + \frac{\Theta Z_2(t)}{C^s}. \quad (15)$$

### III. SIMULATION RESULT AND DISCUSSION

The system parameters that have been used for the simulation are shown in table 1.

Description	Symbol	Value
Aluminum beam dimension	-	80 x 10 x 0.6 mm <sup>3</sup>
Distributed mass of beam	M <sub>b</sub>	1.676 g
Young modulus of beam	E <sub>b</sub>	70 x 10 <sup>9</sup> Nm <sup>-2</sup>
Moment of inertia of beam	I <sub>b</sub>	0.54 mm <sup>4</sup>
Tip mass with magnet	M <sub>t</sub>	2.11 g
Piezoelectric material dimension	-	42 x 7 x 0.3 mm <sup>3</sup>
Moment of inertia of piezoelectric material	I <sub>p</sub>	0.048 mm <sup>4</sup>
Clamp capacitance	C <sup>s</sup>	12.45 x 10 <sup>-9</sup> F
Young modulus of piezoelectric patch	E <sub>p</sub>	30x10 <sup>9</sup> Nm <sup>-2</sup>
Length of magnet	l <sub>m</sub>	3 mm
Diameter of magnet	d <sub>m</sub>	4 mm
Surface flux	$\beta$	1.4 T
Electromechanical coupling coefficient	$\Theta$	1.71x10 <sup>-4</sup> NV <sup>-1</sup>
Permeability of medium	$\tau_0$	4 $\pi$ x 10 <sup>-7</sup> Hm <sup>-1</sup>

**Table 1 : System parameters used for simulation**

All parameters value shown in table 1 are used to determine the value of system parameters that needed in state space equation above using the following relations.

$$M_{eq} = \frac{33}{140} M_b + M_t \quad (16)$$

$$\begin{aligned} K_{eq} &= K_{beam} + K_{patch} \\ &= \left( \frac{3E_b I_b}{L_b} \right)_{beam} \\ &\quad + \left( \frac{3E_p I_p}{L_p} \right)_{patch} \end{aligned} \quad (17)$$

$$C_{eq} = 2\xi M_{eq} \omega_n \quad (18)$$

$$m = \frac{2\beta V}{\tau_0} \quad (19)$$

$$R = \frac{1}{\omega_n C^s} \quad (20)$$

The following fig.4and table 2shows a chart of comparison of performance between the different configuration of PEH and type of configuration used respectively.

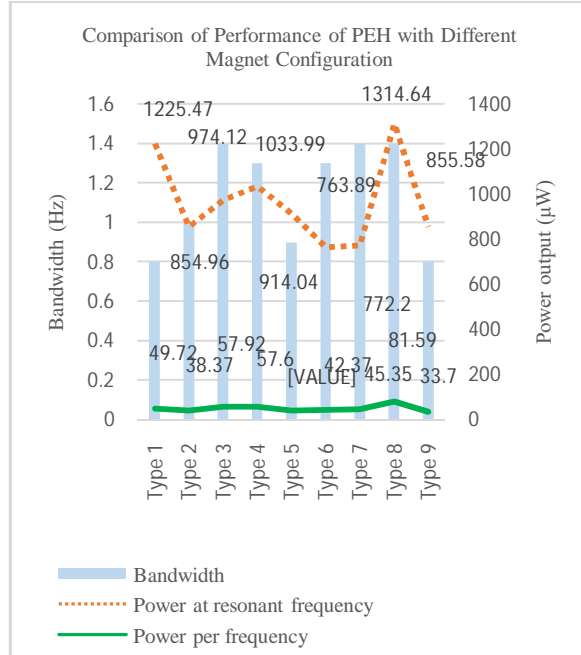


Fig. 4 Chart of performance comparison of PEH with different magnet configuration

	Configuration
Type 1	Conventional PEH (without magnet)
Type 2	PEH with fixed front magnet (attractive) only
Type 3	PEH with fixed front magnet (repulsive) only
Type 4	PEH with fixed top and bottom magnet (attractive) only
Type 5	PEH with fixed top and bottom magnet (repulsive) only
Type 6	PEH with fixed top, bottom and front magnet (attractive)
Type 7	PEH with fixed top, bottom and front magnet (repulsive)
Type 8	PEH with fixed top and bottom magnet (attractive) and front magnet (repulsive)
Type 9	PEH with fixed top and bottom magnet (repulsive) and front magnet (attractive)

Table 2: Different type of configuration of PEH used in simulation

For this simulation, the conventional cantilever beam PEH without using any magnet is made as a benchmark. Each type of PEH configuration is simulated using sweep-up frequency at excitation level of rms acceleration of  $2 \text{ m/s}^2$ . The bandwidth for this simulation is calculated based on half power bandwidth. Moreover, performance of other configuration is compared with the conventional PEH in terms of its difference in bandwidth, resonance frequency, maximum power output at resonance frequency, and power output per frequency. For the power output per frequency, the total summation of power output for each configuration is averaged on

certain range of frequency which is from 5 Hz to 45 Hz. This will be helpful because it provides another way to evaluate the performance of PEH by showing the quality of each configuration. By introducing the magnet interaction into the system, there is some improvement in bandwidth of PEH. From the fig. 4, by adding a fixed front magnet, the bandwidth is increased from 0.8 Hz to 1.4 Hz and from 0.8 Hz to 1 Hz when the magnet is in repulsive and attractive mode respectively even though there is some decrement in maximum power output for both attractive and repulsive mode. But, the power output per frequency is still higher than conventional PEH for PEH with front magnet in repulsive mode which is  $57.92 \mu\text{W}/\text{Hz}$ , 16 percent higher than the PEH without magnet.

In addition, when the fixed top and bottom magnets are added, the bandwidth is still better than the conventional PEH. The bandwidth is increased from 0.8 Hz to 1.3 Hz when in attractive mode and increased slightly from 0.8 Hz to 0.9 Hz when in repulsive mode. Furthermore, when all three magnets, top, bottom and front magnets are included on the system, the simulation results showed that the bandwidth is improved for both attractive and repulsive mode. Unfortunately, when all three magnets are in either attractive mode or repulsive mode, the maximum power at resonance frequency and power per frequency, both are lower than the conventional PEH. Through observation from the result of simulation, the fixed front magnet configuration yields positive effect when it is in repulsive mode while top and bottom magnet configuration yields positive effect when it is in attractive mode. Even though the maximum power output for both configurations are lower than conventional PEH, these two configurations outperform the conventional PEH in both bandwidth and power per frequency.

Thus, by combining these two configurations, where top and bottom magnet in attractive mode and front magnet in repulsive mode, the ideal PEH can be obtained. This is shown by simulation result that there is significant improvement in bandwidth, maximum power output at resonance frequency and power per frequency. The bandwidth is 1.4 Hz while maximum power output and power per frequency is  $1314.64 \mu\text{W}$  and  $81.59 \mu\text{W}/\text{Hz}$  respectively. It is worth to mention that the resonance frequency is much lower than conventional PEH as can be seen in fig. 4. The resonance frequency for combination of top and bottom magnet configuration in attractive mode and front magnet in repulsive mode is 13.8 Hz, 14.2 Hz lower than the conventional PEH frequency and this is preferred as it is suitable to power up devices such as in wireless sensor network where the ambient vibration around the devices is considerably low. Besides, from the fig. 5, it also can be observed that the peak of configuration type 8 is slightly tilted

to the left which indicating the effect of nonlinearity produced by the magnet.

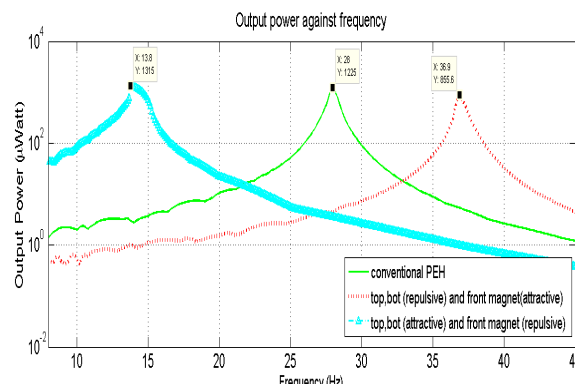


**Fig. 5** Graph of output power vs frequency for type 1, type 8 and type 9 PEH.

## CONCLUSION

In this paper, a piezoelectric based vibration energy harvester with multiple magnet is proposed. The mathematical model describing the system is developed and the best configuration is obtained where the best configuration is when the top and bottom magnet is in attractive mode while the front magnet is in repulsive mode. The simulation results show that the best configuration yields 1.4 Hz bandwidth, and its maximum power output at resonance frequency is 1314.64  $\mu\text{W}$ , 89.17  $\mu\text{W}$  higher than the conventional PEH and has power per frequency of 81.59  $\mu\text{W}/\text{Hz}$ , which is about 64 percent higher than PEH without any magnets. With low resonance frequency at 13.8 Hz, the suggested configuration of PEH is suitable to power up the low power devices by harnessing vibration energy from its surrounding.

## ACKNOWLEDGMENT

This work is supported by Fundamental Research Grant Scheme (FRGS15-165-0406) from the Ministry of Higher Education Malaysia.

## REFERENCES

- [1] E. Murimi and M. Neubauer, "Piezoelectric Energy Harvesting; An Overview," vol. 4, no. 5, pp. 117–121, 2012.
- [2] D. Cavalheiro, F. Moll, and S. Valtchev, "A battery-less, self-sustaining RF energy harvesting circuit with TFETs for  $\mu\text{W}$  power applications," 14th IEEE Int. NEWCAS Conf. NEWCAS 2016, vol. 1, pp. 1–4, 2016.
- [3] S. M. Jung and K. S. Yun, "A wideband energy harvesting device using snap-through buckling for mechanical frequency-up conversion," Proc. IEEE Int. Conf. Micro Electro Mech. Syst., vol. 1, pp. 1207–1210, 2010.
- [4] D. Galayko, A. Dudka, and P. Basset, "Capacitive kinetic energy harvesting: System-level engineering challenges," 2014 21st IEEE Int. Conf. Electron. Circuits Syst. ICECS 2014, pp. 882–885, 2014.
- [5] T. Reissman, E. M. Wolff, and E. Garcia, "Piezoelectric Resonance Shifting Using Tunable Nonlinear Stiffness," Act. Passiv. Smart Struct. Integr. Syst., vol. 7288, p. 72880G-72880G-12, 2009.
- [6] V. R. Challa, M. G. Prasad, and F. T. Fisher, "Towards an autonomous self-tuning vibration energy harvesting device for wireless sensor network applications," Smart Mater. Struct., vol. 20, no. 2, p. 25004, 2011.
- [7] G. A. Muthalif and N. H. D. Nordin, "Optimal piezoelectric beam shape for single and broadband vibration energy harvesting : Modeling , simulation and experimental results," Mech. Syst. Signal Process., pp. 1–10, 2014.
- [8] S. Ben-Yakov, G. Hadar, A. Shainkopf, and N. Kriehely, "A friendly approach to increasing the frequency response of piezoelectric generators," 2013 IEEE 33rd Int. Sci. Conf. Electron. Nanotechnology, ELNANO 2013 - Conf. Proc., pp. 349–353, 2013.
- [9] Y. Jia, S. Du, and A. A. Seshia, "Eight parametric resonances in a multi-frequency wideband MEMS piezoelectric vibration energy harvester," Proc. IEEE Int. Conf. Micro Electro Mech. Syst., vol. 2016–Febru, no. January, pp. 1244–1247, 2016.
- [10] N. Elvin and A. Erturk, Advances in Energy Harvesting Method. 2013.
- [11] G. Zhang, S. Gao, H. Liu, and S. Niu, "A low frequency piezoelectric energy harvester with trapezoidal cantilever beam: theory and experiment," Microsyst. Technol., pp. 1–10, 2016.
- [12] D. S. Ibrahim, A. G. A. Muthalif, N. H. D. Nordin, and T. Saleh, "Comparative study of conventional and magnetically coupled piezoelectric energy harvester to optimize output voltage and bandwidth," Microsyst. Technol., vol. 22, no. 8, pp. 1–12, 2016.
- [13] T. K. Chung, C. M. Wang, P. C. Yeh, T. W. Liu, C. Y. Tseng, and C. C. Chen, "A three-axial frequency-tunable piezoelectric energy harvester using a magnetic-force configuration," IEEE Sens. J., vol. 14, no. 9, pp. 3152–3163, 2014

★ ★ ★